Atmos. Chem. Phys. Discuss., 13, 14823–14869, 2013
www.atmos-chem-phys-discuss.net/13/14823/2013/
doi:10.5194/acpd-13-14823-2013

Atmospheric Chemistry and Physics Discussions
Open Access

Review and uncertainty assessment of size-resolved scavenging coefficient formulations for snow scavenging of atmospheric aerosols

L. Zhang[1], X. Wang[2], M. D. Moran[1], and J. Feng[3]

[1]Air Quality Research Division, Science and Technology Branch, Environment Canada, 4905 Dufferin St, Toronto, Ontario, M3H 5T4, Canada
[2]Kellys Environmental Services, Toronto, Ontario, Canada
[3]Canadian Meteorological Centre, Meteorological Service of Canada, Environment Canada, 2121 Trans-Canada Highway, Dorval, Quebec, H9P 1J3, Canada

Received: 3 April 2013 – Accepted: 17 May 2013 – Published: 5 June 2013

Correspondence to: L. Zhang (leiming.zhang@ec.gc.ca)

Published by Copernicus Publications on behalf of the European Geosciences Union.

Abstract

Theoretical parameterizations for the size-resolved scavenging coefficient for atmospheric aerosol particles scavenged by snow (Λ_{snow}) need assumptions regarding (i) snow particle–aerosol particle collection efficiency E, (ii) snow particle size distribution $N(D_p)$, (iii) snow particle terminal velocity V_{D}, and (iv) snow particle cross-sectional area A. Existing formulas for these parameters are reviewed in the present study and uncertainties in Λ_{snow} caused by various combinations of these parameters are assessed. Different formulations of E can cause uncertainties in Λ_{snow} of more than one order of magnitude for all aerosol sizes for typical snowfall intensities. E is the largest source of uncertainty among all the input parameters, similar to rain scavenging of atmospheric aerosols (Λ_{rain}) as was found in a previous study by Wang et al. (2010). However, other parameters can also cause significant uncertainties in Λ_{snow}, and the uncertainties from these parameters are much larger than for Λ_{rain}. Specifically, different $N(D_{\text{p}})$ formulations can cause one-order-of-magnitude uncertainties in Λ_{snow} for all aerosol sizes, as is also the case for a combination of uncertainties from both V_{D} and A. In comparison, uncertainties in Λ_{rain} from $N(D_{\text{p}})$ are smaller than a factor of 5 and those from V_{D} are smaller than a factor of 2. Λ_{snow} estimated from one empirical formula generated from field measurements falls in the upper range of, or is slightly higher than, theoretically estimated values. The predicted aerosol concentrations obtained using different Λ_{snow} formulas can differ by a factor of two for just a one-centimeter snowfall (liquid water equivalent of approximately 1 mm). It is likely that, for typical rain and snow event the removal of atmospheric aerosol particles by snow is more effective than removal by rain for equivalent precipitation amounts, although a firm conclusion requires much more evidence.

1 Introduction

Many physical and chemical processes in chemical transport models (CTMs) need to be parameterized due to limitations in computer resources and our incomplete knowledge of these processes. For the scavenging and the removal of atmospheric aerosol particles by falling hydrometeors, the scavenging coefficient Λ (s^{-1}), which denotes the fraction of aerosol particles removed per unit time, is typically used when solving aerosol particle mass continuity equations in CTMs (e.g., Baklanov, 1999; Loosmore and Cederwall, 2004; Gong et al., 2006; Henzing et al., 2006; Sofiev et al., 2006; Tost et al., 2006; Feng, 2007; Croft et al., 2009). Many laboratory, field, and theoretical studies have been conducted to quantify Λ under rain and snow conditions (Martin et al., 1980; Slinn, 1984; Murakami et al., 1985; Miller and Wang, 1989; Dick, 1990; Maryon et al., 1992; Sparmacher et al., 1993; Bell and Saunders, 1995; Jylhä, 2000; Rotstayn and Lohmann, 2002; Laakso et al., 2003; Zhang et al., 2004; Chate, 2005; Andronache et al., 2006; Croft et al., 2009; Feng, 2009; Kyrö et al., 2009; Paramonov et al., 2011; Wang et al., 2011). However, large uncertainties still exist in current Λ parameterizations due to the many factors involved in the scavenging processes.

An assessment of uncertainties on size-resolved Λ for aerosols scavenged by rain (Λ_{rain}) was recently conducted by Wang et al. (2010). The present study follows a similar approach to assess uncertainties of size-resolved Λ for aerosols scavenged by snow (Λ_{snow}). Such a study is needed given that current knowledge of snow scavenging is considerably more limited than that for rain scavenging. One reason is that scavenging by snow is more complicated due to the wide variety of snow particle shapes, sizes, and densities, which results in different fall speeds, cross-sectional areas, and flow patterns around snow particles (Pruppacher and Klett, 1997; Jylhä, 1999). On the other hand, snow scavenging is an important removal mechanism in mid-latitude and polar regions in the winter and in mountainous areas and in the upper troposphere at all times of year. One study estimated that roughly 30 % of below-cloud scavenging of sulphate particles by precipitation is due to snow (Croft et al., 2009).

Current treatments of snow scavenging of atmospheric aerosol particles in CTMs vary substantially, ranging from using a bulk Λ parameterized as a function of snowfall intensity (as liquid water equivalent) without considering the sizes of either aerosol or snow particles (Baklanov, 1999; Sofiev et al., 2006) to using the same size-resolved Λ formula as that for rain scavenging to using a size-resolved Λ formula specifically developed for snow conditions (e.g., Gong et al., 2006; Croft et al., 2009; Feng, 2009). Past reviews have documented these various approaches (Rasch et al., 2000; Textor et al., 2006; Sportisse, 2007; Zhang, 2008; Gong et al., 2011). The present study, however, attempts to quantify the uncertainties related to various parameters chosen for the existing size-resolved Λ_{snow} formulas developed specifically for snow conditions.

In the following sections, a brief overview of current size-resolved Λ_{snow} parameterizations, including their component parameters, is first given (Sect. 2); next, a summary of the results of sensitivity tests that were conducted to investigate uncertainties in Λ_{snow} induced by these various parameters is provided (Sect. 3). The uncertainties of existing theoretical size-resolved Λ_{snow} parameterizations is then assessed further by using various combinations of the component parameter formulas (Sect. 4.1) and by comparing with an available empirical Λ_{snow} parameterization derived directly from fits to field measurements (Sect. 4.2). The impact of different Λ_{snow} formulas on predicted aerosol concentrations is then briefly discussed (Sect. 4.3) and a comparison of uncertainties between Λ_{snow} and Λ_{rain} is presented (Sect. 4.4). Lastly, some conclusions are given in Sect. 5.

2 Theory of size-resolved snow scavenging coefficient Λ_{snow}

The terminology of ice or snow particles reflects the greater physical variability of frozen or solid hydrometeors vs. liquid hydrometeors (rain drops). As discussed by Pruppacher and Klett (1997), small ice particles that have grown only by water vapour diffusion are called ice crystals or snow crystals. These crystals have different shapes or habits, including plates, columns, stars, needles, dendrites, spheres, and bullets. Ag-

ACPD
13, 14823–14869, 2013

gregates of snow crystals are called snowflakes. Individual snow crystals usually have a maximum dimension D_m of less than 5 mm whereas snowflakes may have a maximum dimension of several cm. Snow crystals can also grow by collisions with cloud drops, which is called riming. Depending upon the degree of riming, these snow particles may be referred to as rimed snow crystals or graupel particles or ice pellets. All of these rimed snow particles usually have D_m values of less than 5 mm; heavily-rimed larger particles are called hailstones.

In CTMs that simulate aerosol particle number concentrations, the below-cloud scavenging of aerosol particles by snow is commonly described as (Seinfeld and Pandis, 2006)

$$\frac{\partial n(d_p,t)}{\partial t} = -\Lambda_{snow}(d_p)\cdot n(d_p,t) \tag{1}$$

where $n(d_p,t)$ is the number concentration of aerosol particles with diameters d_p at time t, and $\Lambda_{snow}(d_p)$ is the scavenging coefficient for aerosol particles of size d_p and can be calculated based on the concept of collection efficiency between falling hydrometeors and aerosol particles (e.g., Slinn, 1984). The size-resolved scavenging coefficient is parameterized as

$$\Lambda_{snow}(d_p) = \int_0^\infty A(V_D - v_d)E(d_p,D_p)N(D_p)\mathrm{d}D_p \tag{2}$$

where $N(D_p)\mathrm{d}D_p$ is the number of snow particles with a melted diameter between D_p to $D_p+\mathrm{d}D_p$ in a unit volume of air (m^{-3}), V_D and v_d are the terminal velocities ($m\,s^{-1}$) of snow particles and aerosol particles, respectively, $E(d_p,D_p)$ is the collection efficiency (dimensionless) between an aerosol particle of size d_p and a snow particle of size D_p, and A is the effective cross-sectional area of a snow particle projected normal to the fall direction (m^2). According to Eq. (2), four parameters determine the value of $\Lambda_{snow}(d_p)$: (i) the snow particle–aerosol particle collection efficiency; (ii) the snow-particle number

ACPD
13, 14823–14869, 2013

size distribution; (iii) the snow-particle terminal velocity (assuming $V_D \gg v_d$); and (iv) the snow-particle effective cross-sectional area. Available formulas for these four parameters are reviewed and discussed below. All symbols used in this study are defined in Table A1.

2.1 Snow particle–aerosol particle collection efficiency $E(d_p, D_p)$

$E(d_p, D_p)$, the collection efficiency for aerosol particles of diameter d_p of a snow particle of melted diameter D_p, gives the rate of collection of aerosol particles of diameter d_p by the falling snow particle normalized by the number of upstream particles of diameter d_p swept across an area equal to the effective cross-sectional area of the snow particle (e.g., Slinn, 1984). The collection efficiency is the most important parameter in the calculation of Λ_{snow} in Eq. (2). There are considerably fewer studies on E for snow particles and aerosol particles than there are for rain drops and aerosol particles. However, there are a few studies that describe E based on rigorous theoretical models involving (i) a particle trajectory model under the influence of the flow field of falling ice crystals and (ii) a convective diffusion model for small aerosol particles. For example, Martin et al. (1980) studied E for planar ice crystals (approximated as hexagonal plates) at low-to-intermediate Reynolds numbers and Miller and Wang (1989) studied E for columnar ice crystals using a theoretical model. Several field measurements and laboratory experiments under controlled conditions have also been conducted to study and verify theoretical results (e.g., Knutson et al., 1976; Sauter and Wang, 1989; Murakami et al., 1985). These studies suggest that a complete theoretical model for E would be too complex to be implemented in CTMs. Three different size-resolved semi-empirical formulas for E have thus been developed for CTM applications (Slinn, 1984; Murakami et al., 1985; Dick, 1990) as listed in Table 1. Some of these formulas for E have been used to parameterize Λ_{snow} in current CTMs (e.g., Gong et al., 2006; Croft et al., 2009; Feng, 2009).

2.2 Snow particle number size distribution $N(D_p)$

Λ_{snow} also depends on the number size spectrum of snow particles. Various microphysical and dynamical processes inside and below cloud layers modify snow-particle size spectra. Other factors affecting snow-particle size spectra include ambient temperature, particle habit, precipitation intensity, and the stage of cloud and precipitation development (e.g., Harimaya et al., 2004; Woods et al., 2008). In practical applications, empirical mathematical formulas derived from the observed size spectra have been used to approximate natural snow-particle size distributions (e.g., Marshall and Palmer, 1948; Gunn and Marshall, 1958; Sekhon and Srivastava, 1970; Scott, 1982; Smith, 1984; Mitchell, 1991; Heymsfield, 2003; Field et al., 2005; Woods et al., 2008). For example, the exponential Marshall–Palmer size distribution (Marshall and Palmer, 1948), originally proposed for raindrop size distribution, was also found to describe snow particle size distribution reasonably well (Passarelli, 1978). Gunn and Marshall (1958) reported another exponential size distribution function for aggregate snowflakes, the first one to be derived directly from ground observations of snow, following an assessment method similar to that used for raindrop size distributions by Marshall and Palmer (1948). By reanalyzing the dataset of Gunn and Marshall (1958) as well as analyzing additional snowflake size distribution measurements, Sekhon and Srivastava (1970) suggested an updated exponential formula. Scott (1982) modified the parameters in the Marshall–Palmer distribution based on results from Passarelli (1978) and Houze et al. (1979) so the modified exponential function can be applied to large spatial scales. To date, exponential distributions have been widely used in various cloud microphysics to represent snow size spectra (e.g., Cotton et al., 1982; Lin et al., 1983; Rutledge and Hobbs, 1983; Reisner et al., 1998; Thompson et al., 2004; Croft et al., 2009; Feng, 2009; Solomon et al., 2009).

The basic form of the exponential function for snow particle number size distribution is written as

$$N(D_p) = N_{0e} \exp\left(-\beta_e D_p\right) \tag{3}$$

ACPD
13, 14823–14869, 2013

where N_{0e} is the intercept parameter and β_e is a slope parameter. Different researchers, however, have treated N_{0e} and β_e in different ways, some have adopted a fixed N_{0e} whereas others have varied N_{0e} according to precipitation intensity (Table 2). Note that the parameters in Scott (1982) are based on actual snow particle size D_m whereas the other three distributions listed in Table 2 are for equivalent drop sizes D_p. A conversion of snow particle size to equivalent melted drop size is needed for the Scott (1982) formula (see Appendix A) to allow a direct comparison of these distributions (see Sect. 3.2).

2.3 Snow particle terminal velocity V_D

Terminal velocities for various ice particle types have been studied both experimentally and theoretically, and corresponding empirical parameterizations have been developed (e.g., Langleben, 1954; Pruppacher and Klett, 1997; Mitchell, 1996; Mitchell and Heymsfield, 2005). Early formulas for snow particle terminal velocity were derived directly from fall speed measurements (i.e., experimentally based) and treated the terminal velocity V_D as a power-law function of the ice particle maximum dimension D_m: that is, $V_D = a_v D_m^{b_v}$, where a_v and b_v are empirical constants but varying with ice crystal habit (e.g., Langleben, 1954; Starr and Cox, 1985). However, the application of most experimentally-based empirical formulas is limited to the particle shape for which the measurements were conducted (see Table 3). More recently developed parameterizations are theoretically-based formulas. A power-law relationship is first determined between the Reynolds number (Re; dimensionless) and the Best or Davies number ($X = \frac{2mg\rho_a D_m^2}{A\mu_a^2}$; dimensionless) (Bohm, 1989, 1992; Mitchell, 1996); the terminal velocity is then derived from Re that is determined in terms of X. The detailed description of generating X and the empirical relationship of Re–X were given in Mitchell (1996) and Mitchell and Heymsfield (2005). Since X is a function of the ice particle mass (m) and the cross-sectional area (A), both of which are parameterized as a power-law function of the maximum dimension of the ice particle (D_m), the selection of different power-law

ACPD
13, 14823–14869, 2013

Assessment of scavenging coefficient formulations

L. Zhang et al.

functions for m and A may lead to large differences in the X value, and thus to large errors in V_D (Mitchell, 1996). The advantage of the theoretically-based parameterizations, however, is that they can be applied to any particle shape (Table 3).

2.4 Snow particle cross-sectional area A

Knowledge of the cross-sectional area of a snow particle is essential for accurate calculation of Λ_{snow} and for the estimation of snow particle terminal velocity. Snow particles can have dozens of irregular shapes and it is not realistic to represent the A of all particle shapes accurately using one single theoretical formula. A common approach associating A of a snow particle and its mass (m) is through the definition of a parameter: the particle's maximum dimension, D_m. Both m and A are parameterized as power-law functions of D_m: $m = \alpha D_m^{\beta}$ and $A = \gamma D_m^{\sigma}$, where α, β, γ, and σ are empirical constants developed from measurements of natural snow particles (e.g., Locatelli and Hobbs, 1974; Mitchell et al., 1990; Mitchell and Arnott, 1994; Mitchell, 1996; Pruppacher and Klett, 1997; Woods et al., 2008). The detailed empirical expressions and related parameters for various snow types were reviewed by Mitchell (1996).

In the present study, four habit types of snow crystals – spherical ice crystal, dendrite snow plate, columnar ice crystal, and graupel particle – were chosen for analysis and discussion (Table 4). These are the four habits of snow crystals that occur most frequently as revealed by ground observations (Hobbs et al., 1972); they are believed to be the main habits of ice crystals based on the classification of habit composition as determined from the airborne 2D-C probe imagery and ground-based stereomicroscope observations (Woods et al., 2008). As well, current cloud-scale CTMs and numerical weather prediction models only explicitly distinguish and predict a few types of ice crystals, including dendrite snowflake, columnar crystal, and graupel (hail) (e.g., Field and Heymsfield, 2003; Thompson et al., 2008; Morrison et al., 2009).

Note that the particle size D_m used in the diameter-based mass and area power law formulas shown in Table 4 is the maximum dimension for a frozen particle. These relationships can also be represented in terms of D_p, the equivalent drop diameter of

ACPD
13, 14823–14869, 2013

a snow particle when it melts. The melted mass of a snow particle can be expressed in terms of the diameter of its equivalent water drop as

$$m = \rho_{\text{water}} \frac{\pi}{6} D_{\text{p}}^3 \tag{4}$$

where ρ_{water} is the water density. The cross-sectional area of a falling snow particle can then be written as

$$A = \gamma \left(\frac{\rho_{\text{water}} \pi D_{\text{p}}^3}{6\alpha} \right)^{\frac{\sigma}{\beta}} \tag{5}$$

3 Sensitivity of theoretical size-resolved Λ_{snow} to input-parameter selections

From Sect. 2 we know that four component parameters determine Λ_{snow} values and that different formulas have been proposed in the literature for these parameters (see Tables 1–4). The sensitivity of Λ_{snow} to the choice of one of these different formulas for each of these component parameters are discussed below. Note that for all of the sensitivity tests, the temperature and pressure were assumed to be −10 °C and 1013.5 hPa, respectively.

3.1 Sensitivity of Λ_{snow} to E

Figure 1 compares collection efficiencies $E(d_{\text{p}}, D_{\text{p}})$ based on the three formulas listed in Table 1 across the aerosol particle diameter range from 0.001 µm to 10 µm for collection by monodisperse snow particles with four different shapes and three different maximum sizes D_{m}. Each colour in Fig. 1 represents one formula listed in Table 1, and the different symbols on the lines distinguish the four different snow particle shapes (Table 4). A strong dependence of E on aerosol particle size is found for all cases. The ultrafine particles ($d_{\text{p}} < 0.01$ µm) and large particles ($d_{\text{p}} > 3$ µm) have the largest E values while particles with d_{p} around 0.1 µm have the smallest E values. This variation is certainly caused by the size-dependence of the collection mechanisms, namely Brownian diffusion, interception, and inertial impaction, considered in the formulas in Table 1. The contribution of Brownian diffusion to E dominates for the ultrafine particles but decreases rapidly as particle size increases; the contribution of inertial impaction becomes significant when the diameter of an aerosol particle is larger than a few microns; and the contribution of the interception mechanism increases with increasing particle size and appears to be important for particles in the diameter range from 1.0 µm to a few microns. The combined contributions of the three mechanisms lead to low E values for particles in the size range 0.01 µm < d_p < 1.0 µm. Note that other potential collection mechanisms such as diffusiophoresis, thermophoresis, and electric charges are not included in these formulas. For rain scavenging of atmospheric aerosols, these several mechanisms are less important than the three major mechanisms discussed above and are only significant for particles in the size range of 0.01 µm–1.0 µm (Wang et al., 2010; Santachiara et al., 2012). This is also expected to be the case for snow scavenging of aerosols.

It is evident from Fig. 1 that the $E(d_p)$ profiles for fixed D_m from the Murakami et al. (1985) and Dick (1990) formulas are not very sensitive to the snow particle shapes. The four $E(d_p)$ profiles for four snow particle shapes based on the same formula are similar, e.g., all have a minimum E value at the same particle diameter. $E(d_p)$ values for these two formulas also differ only by a factor of 2 to 3 between different snow particle shapes across the entire aerosol particle size range. Note that all of the formulas in Table 1 depend on snow particle terminal velocity V_D either directly or through the Reynolds and Stokes numbers. In the sensitivity tests presented in Fig. 1, V_D values were calculated for all snow-particle habits based on the theoretical formula developed by Mitchell and Heymsfield (2005) (see Table 3; the details of the V_D calculation will be discussed later in Sect. 3.3). Since different snow particle shapes have different A and m values (Table 4), this leads to different Reynolds number Re and different Best or Davies number values, and thus to different V_D values, which caused the small differences in $E(d_p)$. In contrast, the $E(d_p)$ profiles for fixed D_m from the Slinn (1984) formula

ACPD
13, 14823–14869, 2013

showed a different pattern. The $E(d_p)$ profiles for the dendrite and column snow particle shapes are basically the same and the $E(d_p)$ profiles for the sphere and graupel particle shapes are also similar. However, the $E(d_p)$ profiles between these two groups differ significantly, especially for the aerosol particle sizes where the minimum E value occurs. This is due to values specified for two of the parameters used in Slinn's formula (see Table 1); λ and α were given as 10.0 µm and 1.0, respectively, for dendrite and column shapes but 100.0 µm and 2/3, respectively, for sphere and graupel shapes.

Differences in E between the Murakami et al. (1985) and Dick (1990) formulas are significant for all aerosol particle sizes and for all snow particle sizes and shapes considered here. The largest differences occur for particle diameters around 0.1 µm, for which the difference can be larger than one order of magnitude. E decreases significantly with increasing collector (i.e., snow particle) size in these two formulas. The difference in E between these two formulas also decreases with increasing collector size. The dependence of E on collector size is because larger collectors have larger V_D values, and thus larger Re values, which results in smaller E values (see formulas in Table 1). Comparing E values for the Slinn (1984) formula with those from the Murakami et al. (1985) and Dick (1990) formulas, the differences are even larger, especially for smaller collectors (e.g., Fig. 1a). Differences up to nearly three orders of magnitude can be seen for aerosol particle sizes from 0.1 µm to 2 µm. It should be pointed out that the E values for the Slinn (1984) formula do not change much with collector size because λ and α values are fixed for all collector sizes, a different behaviour from the other two formulas discussed above.

The sensitivity of Λ_{snow}, calculated using Eq. (2), to the choice of the three different formulas for E (Table 1) is illustrated in Fig. 2 for two snowfall intensity conditions (as liquid water equivalent): 0.1 mm h^{-1} (solid line) and 10 mm h^{-1} (symbol line). The snow particle terminal velocity used for Fig. 2 was that of Mitchell and Heymsfield (2005) (see Table 3) and the snow particle size spectrum followed Sekhon and Srivastava (1970) (see Table 2). Figure 2 indicates that the differences in Λ_{snow} due to the different $E(d_p, D_p)$ formulas vary with aerosol particle size, snow particle shape, and snowfall intensity. For the largest aerosol particles (i.e., $d_p > 10.0\,\mu m$), the differences in Λ_{snow} are small (e.g., a factor of 2) for both snowfall intensities and all snow particle shapes due to the very similar E values in this aerosol particle size range (close to unity; not shown in Fig. 1). For aerosol particles smaller than $10\,\mu m$, a difference of one order of magnitude or larger is seen under all snowfall intensity and snow particle shape conditions. It can also be seen that the differences in Λ_{snow} are smaller for aerosol particles smaller than $0.01\,\mu m$ than for particles between $0.01\,\mu m$–$10.0\,\mu m$, consistent with the differences in E profiles shown in Fig. 1.

Figure 2 also suggests that Λ_{snow} values derived from the Murakami et al. (1985) and Dick (1990) formulas agree well (e.g., within a factor of 2) for aerosol particles larger than $1.0\,\mu m$ and differ by a factor of 3 to 4 for aerosol particles smaller than $0.1\,\mu m$ for all snow shapes and snowfall intensities. In contrast, Λ_{snow} values from the Slinn (1984) formula shows a large deviation from those of the other two formulas, in particular for the aerosol particle size range of $0.1\,\mu m < d_p < 10.0\,\mu m$, except for the case for dendrites and a light snowfall intensity. Again, this can be explained by the E pattern shown in Fig. 1. These results suggest that the formulation used to describe the collection efficiency is a very important source of uncertainty in estimating Λ_{snow}.

3.2 Sensitivity of Λ_{snow} to $N(D_p)$

Snow particle size distributions ($N(D_p)$) generated from the four widely used exponential formulas listed in Table 2 are shown in Fig. 3 for two snowfall intensities (as liquid water equivalent): 0.1 and $1.0\,mm\,h^{-1}$. The Gunn–Marshall (GM) and the Sekhon–Srivastava (SS) $N(D_p)$ profiles are quite close due to their similar values for the intercept parameter N_{0e} and slope parameters β_e (see Table 2). The Marshall–Palmer (MP) distribution differs significantly from those of GM and SS, and the Scott (SC) distribution is even more different. All four exponential distributions yield large numbers of small snow particles (< 0.1 mm). This is due to the limitation in the definition of the exponential formula, which generally predicts maximum number concentration for particle sizes approaching zero (see Eq. 3).

ACPD
13, 14823–14869, 2013

The percentages of snow particle number concentrations in different size ranges are shown in Table 5 for three of the four snow-particle size distributions and four snowfall intensities. Note that N_{0e} is fixed for the MP and SC distributions but decreases with increasing snowfall intensity for the SS distribution (see Table 2). Thus, the total snow particle number concentrations from the MP and SC distributions increase and those from the SS decrease with increasing snowfall intensity (Table 5). The total number concentrations from different size distributions can differ from less than one order of magnitude to more than two orders of magnitude, depending on snowfall intensity. For all of the size distributions, however, the percentages of the smallest snow particles (< 0.1 mm) decrease and those of the largest snow particles (> 1 mm) increase with increasing snowfall intensity. This can also be seen from Fig. 3, in which all of the snow-particle size distribution profiles shift to larger snow particle sizes with increasing snowfall intensity.

Figure 4 shows the sensitivity of Λ_{snow} to the four different snow particle number size distributions $N(D_p)$ considered in Fig. 3 for four snow particle shapes and two snowfall intensities (as liquid water equivalent): 0.1 mm h^{-1} and 10 mm h^{-1}. V_D and $E(d_p, D_p)$ were assumed to follow the theoretical formulas of Mitchell and Heymsfield (2005) and Murakami et al. (1985), respectively. Differences in Λ_{snow} values derived from these different $N(D_p)$ formulas are up to one order of magnitude for all aerosol particle sizes under light snowfall intensity (0.1 mm h^{-1}). The differences in Λ_{snow} also increase with increasing snowfall intensity and can be larger than one order of magnitude for very strong snowfall intensity (e.g., 10 mm h^{-1}). The dependence of Λ_{snow} on snowfall intensity is also greater for some $N(D_p)$ formulas than others. Based on the Λ_{snow} profiles shown in Fig. 4, we can conclude that in general different assumptions for $N(D_p)$ contribute an uncertainty to the Λ_{snow} profile of about one order of magnitude for all aerosol particle sizes under all snow particle shape and snowfall intensity conditions.

3.3 Sensitivity of Λ_{snow} to V_{D} and A

Figure 5a shows the terminal velocities V_{D} of snow particles with four different shapes calculated from empirical and theoretical formulas selected from Table 3. Each colour represents one particle shape and each symbol represents one formula. Note that the theoretical formula of Mitchell and Heymsfield (2005) was considered to apply to any kind of snow particle shape. Results from the theoretical formula of Mitchell (1996) are not shown in the figure because the calculated values are quite close to those from Mitchell and Heymsfield (2005). For snow particles larger than 0.2 mm, V_{D} values for the same particle shape but based on different formulas are generally within a factor of 5; however, the differences can be larger than a factor of 10 if considering both different particle shapes and different formulas. For snow particles smaller than 0.2 mm, the differences in V_{D} can be up to two orders of magnitude and generally increase rapidly with decreasing snow particle size. As well, V_{D} values from all of the empirical formulas are larger than those from the theoretical formula of Mitchell and Heymsfield (2005) for all particle shapes. The best agreement between the empirical and theoretical formulas is for the dendrite shape and snow particles larger than 0.2 mm.

Figure 5b shows the cross-sectional area A of a snow particle versus its maximum dimension for four different snow particle shapes based on the power-law formulas listed in Table 4. The differences in A between different snow particle shapes increases from a factor of 3 to a factor of more than 10 as snow particle size increases from 0.1 to 10 mm.

The results of sensitivity tests conducted to investigate the influence of V_{D} and A on Λ_{snow} for four different snow particle shapes and three different snowfall intensities (0.1, 1.0 and 10 mm h^{-1} as liquid water equivalent) are shown in Fig. 6. Λ_{snow} profiles were calculated for the nine V_{D} profiles shown in Fig. 5a and the four A profiles shown in Fig. 5b for each snowfall intensity. All of the sensitivity tests shown in this figure used the snow particle size spectrum formula of Sekhon and Srivastava (1970) (Table 2) and the collection efficiency formula of Murakami et al. (1985) (Table 1). As in Fig. 5a,

ACPD
13, 14823–14869, 2013

each colour in Fig. 6 represents one snow particle shape and each symbol represents one V_D formula. It is also evident from Fig. 5b that each snow particle shape only has one formula available for A. Thus, the influence of V_D on Λ_{snow} can be identified by comparing Λ_{snow} profiles for the same snow particle shape (i.e., same coloured lines), while the influence of A on Λ_{snow} can be identified by comparing Λ_{snow} profiles based on the same V_D formula (e.g., the four lines using the formula of Mitchell and Heymsfield, 2005). The overall uncertainty in the Λ_{snow} profile shown in Fig. 6 is thus due to the combination of influences from both V_D and A.

Figure 6 shows that Λ_{snow} may vary by a factor of 2 to 3 for the same snow particle shape for all aerosol particle sizes if different V_D formulas are used, and it may also vary by a factor of 2 to 3 for different snow particle shapes even for the same V_D formula. The combined uncertainties from both V_D and A can thus be as high as a factor of 10. Λ_{snow} values also increase with increasing snowfall intensity, as do the uncertainties in Λ_{snow} values. While the uncertainty in Λ_{snow} caused by uncertainties in either V_D or A are smaller than those associated with the representation of $E(d_p, D_p)$ or $N(D_p)$, the combined uncertainty due to V_D and A can be comparable to the other two factors in some cases, e.g., for large aerosol particles and for strong snowfall intensity (e.g., compare Fig. 6c with Fig. 2). It is also worth noting that the uncertainties in Λ caused by V_D are larger for the snow conditions discussed here than for the rain conditions discussed in Wang et al. (2010), and the largest uncertainties under snow conditions are for large aerosol particles vs. submicron aerosol particles under rain conditions. Thus, significant differences exist in the uncertainties associated with Λ between rain and snow conditions.

ACPD
13, 14823–14869, 2013

4 Assessment of size-resolved Λ_{snow} parameterizations

4.1 Uncertainties in theoretical estimates of size-resolved Λ_{snow} profiles

As discussed in the previous sections, theoretically-based parameterizations of Λ_{snow} require knowledge of $E(d_p, D_p)$, $N(D_p)$, V_D, and A. However, due to the natural variability of snow particle shapes and densities, the limited experimental evidence, and the complexity of microphysical collection processes, there has not been any agreement or consensus in the modelling community as to which formulas should be used for the above-mentioned component parameters in the calculation of Λ_{snow}. For example, Feng (2009) proposed a size-resolved model for below-cloud snow scavenging, in which $E(d_p, D_p)$ was based on a combination of schemes by Martin et al. (1980), Miller and Wang (1989), and Murakami et al. (1985), $N(D_p)$ followed Sekhon and Srivastava (1970), and V_D and A followed Mitchell (1996). Croft et al. (2009) also proposed a size-resolved parameterization for below-cloud snow scavenging, in which E followed Dick (1990) or Slinn (1984), but all snow particles were assumed to be 30 µg in mass and 0.5 mm in radius and to fall at 80 cm s^{-1}. Gong et al. (2006) parameterized aerosol scavenging by snow based on the Slinn (1984) formula for E and assuming a stellar shape for snow crystals when $-25\,^{\circ}\mathrm{C} < T < 0\,^{\circ}\mathrm{C}$ and a graupel shape when $T < -25\,^{\circ}\mathrm{C}$.

In this section, the uncertainties in existing theoretical size-resolved Λ_{snow} parameterizations were investigated using various combinations of the available formulas for the above-mentioned component parameters. Three semi-empirical formulas for $E(d_p, D_p)$ (Slinn, 1984; Murakami et al., 1985; and Dick, 1990; see Table 1 and Sect. 2.1) and three formulas for $N(D_p)$ (SS – Sekhon and Srivastava (1970); SC – Scott (1982); and MP – Marshall and Palmer (1948); see Table 2 and Sect. 2.2) were combined together to generate nine sensitivity tests for each of four snow particle shapes (Fig. 7). The V_D formula of Mitchell and Heymsfield (2005) was used in every sensitivity test because this is the only formula applicable to all snow particle shapes. This formula is a physically-based parameterization and it seems to predict more reasonable V_D values for small snow particles (i.e., $D_m < 0.5$ mm) than empirically-based formulas (see Sect. 3.3). Besides, the uncertainty in Λ_{snow} values due to the specification of V_{D} is much smaller than those introduced by the specification of $E(d_{\text{p}}, D_{\text{p}})$ and $N(D_{\text{p}})$ (Sect. 3.3). Note that uncertainties from various A formulas are implicitly included in different snow particle shapes, as can be seen by comparing the four panels in both Fig. 7 and Fig. 8.

Under light snowfall intensities (e.g., 0.1 mm h^{-1} in Fig. 7), the uncertainties in the calculated Λ_{snow} are generally in the range of one to two orders of magnitude for very small (e.g., < 0.01 µm) and very large (e.g., > 10 µm) aerosol particles. The uncertainties are much larger for the median size aerosols, i.e., two orders of magnitude or more. The largest uncertainty occurs at an aerosol particle size of around 0.1 µm for dendrite and column habits and at an aerosol particle size of around 1 µm for sphere and graupel habits. This difference is largely associated with snow particle shape caused by the differences in $E(d_{\text{p}}, D_{\text{p}})$ profiles for different snow particle shapes as shown in Fig. 2. The ranges of Λ_{snow} values for any aerosol particle size are also different for different snow particle shapes as can be seen by comparing the four Fig. 7 panels, which is due in part to the impact of different A formulas on the calculated Λ_{snow} values.

It was shown in Sect. 3 that, for a snowfall intensity (as liquid water equivalent) of 0.1 mm h^{-1}, different $E(d_{\text{p}}, D_{\text{p}})$ formulas can cause uncertainties in Λ_{snow} of one to two orders of magnitude and different $N(D_{\text{p}})$ formulas can cause uncertainties in Λ_{snow} of one order of magnitude, depending on aerosol particle size. As shown in Fig. 7, the combined uncertainties from both $E(d_{\text{p}}, D_{\text{p}})$ and $N(D_{\text{p}})$ are larger than those caused by the individual parameters. Thus, the uncertainties in Λ_{snow} values from each individual parameter can either cancel each other (i.e., profiles close together) or enhance each other (i.e., profiles further apart).

Figure 8 shows a similar comparison to Fig. 7 for a snowfall intensity of 1 mm h^{-1}. When snowfall intensity increases, Λ_{snow} values also increase for all aerosol particle sizes (compare Fig. 8 with Fig. 7; note the different scales for the y-axes), as do uncertainties in the Λ_{snow} values. The increases in uncertainty are larger for small aerosol particles (0.001–0.1 µm) than for large particles. Apparently, some formulas are more

ACPD
13, 14823–14869, 2013

sensitive to snowfall intensity than others are for smaller aerosol particles. The uncertainties in Λ_{snow} can be as high as two orders of magnitude even for very small aerosol particles (e.g., 0.001 µm). From Sect. 3.2 it is known that the differences in the total number of snow particles between different $N(D_p)$ formulas increase with increasing snowfall intensity. This behaviour at least partly explains the increased uncertainties in Λ_{snow} with decreasing aerosol particle size.

4.2 Comparison between theoretically- and empirically-estimated Λ_{snow} profiles

Λ_{snow} values calculated using the empirical formula of Paramonov et al. (2011) (Appendix B) are also shown in Figs. 7 and 8 (pink curves). The formula was developed based on the empirical fit to four years of field measurements in an urban environment in Finland and applies to a variety of different snow particle shapes (e.g., snowflakes, snow grains, ice crystals, ice pellets, and mixed snow and rain). Although the urban field data covered a range of snowfall intensities (as liquid water equivalent) from 0.1 to 1.2 $mm\,h^{-1}$, the Λ_{snow} values in the formula of Paramonov et al. (2011) do not depend on snowfall intensity or snow particle shape. Therefore, the same pink curve is plotted in each panel of Figs. 7 and 8. Note that this empirical formula is only valid for aerosol particle sizes of 0.01–1.0 µm. It should also be noted that there was another formula in the literature which was developed by Kyrö et al. (2009) based on four years of field data collected in a rural background environment; but the formula was only applicable to light snow intensities and thus was not compared here.

Λ_{snow} values from this empirical formula are several times larger than the upper range of the theoretically-estimated values for a light snowfall intensity (Fig. 7) but are within the upper range of the theoretically-estimated values for a strong snowfall intensity (Fig. 8) for aerosol particles of diameter 0.01–1.0 µm. As mentioned above, the empirical formula was based on measurements spanning snowfall intensities from 0.1 to 1.2 $mm\,h^{-1}$. If the snowfall intensities during the experiment were equally likely, then since Λ_{snow} should vary directly with snowfall intensity (e.g., a factor of 5 larger for 1.0 $mm\,h^{-1}$ than for 0.1 $mm\,h^{-1}$ as shown from the theoretically-based Λ_{snow} profiles

Discussion Paper | Discussion Paper | Discussion Paper | Discussion Paper |
ACPD
13, 14823–14869, 2013
Assessment of scavenging coefficient formulations
L. Zhang et al.

in Figs. 7 and 8), the empirical Λ_{snow} formula should overpredict Λ_{snow} for a snowfall intensity of 0.1 mm h^{-1} but slightly underpredict Λ_{snow} for a snowfall intensity of 1.0 mm h^{-1}. Thus, the empirical profiles should shift down to smaller values in Fig. 7 and shift up to larger values in Fig. 8. This adjustment suggests that the empirically-estimated Λ_{snow} profiles are in the upper range of, or are just slightly larger than, the theoretically-estimated values for all aerosol particle sizes and snowfall intensities for which the empirical formula applies.

4.3 Impact of Λ_{snow} uncertainties on predicted aerosol concentrations

Following Wang et al. (2010), two aerosol particle size distributions, representing marine and urban aerosol populations, respectively, were taken as examples to investigate the impact of different Λ parameterizations on predicted aerosol particle concentrations under two snowfall intensities (0.1 mm h^{-1} and 1.0 mm h^{-1}, as liquid water equivalent). The initial size distribution for each aerosol type was described as a sum of three log-normal functions. Three Λ_{snow} parameterizations shown in Figs. 7 and 8 (MP+MH+SL representing lowest theoretical Λ_{snow}, SC+MH+MU representing highest theoretical Λ_{snow}, and the empirical Λ_{snow} of Paramonov et al., 2011) were chosen to be applied to Eq. (1). The time evolution of the particle number and mass concentrations was then calculated by integrating Eq. (1) with very small time steps (10 s) and a large number of size bins (100) to a time of reaching a total precipitation amount of 5 mm (Fig. 9).

As shown in Fig. 9, significant differences in the bulk number and mass concentrations were found from using different Λ_{snow} formulas. In less than one hour of a typical snowfall intensity (e.g., 1.0 mm h^{-1} as liquid water equivalent, which is approximately 1 cm h^{-1} of snow depth, second row in Fig. 9), a factor of 2 differences were found in both number and mass concentrations for both marine and urban aerosol distributions. It is also clear from Fig. 9 that the impacts of using different Λ_{snow} parameterizations are quantitatively different for the bulk number and mass concentrations. This is because the bulk number concentration is associated with small particles whereas the bulk mass concentration is generally associated with large particles, as can be seen from the initial particle size distributions shown in Fig. 10 in Wang et al. (2010).

4.4 Comparison between Λ_{snow} and Λ_{rain}

Comparing the uncertainties for Λ_{snow} that have been reviewed in this study with those for Λ_{rain} that were reviewed in a previous study (Wang et al., 2010), both similarities and differences were found in terms of the uncertainties caused by various input parameters. For both Λ_{snow} and Λ_{rain}, the formulation of the collection efficiency E between hydrometeors and aerosol particles is the largest source of uncertainty amongst all of the input parameters. The uncertainties in Λ_{snow} and Λ_{rain} caused by E can be more than one order of magnitude for almost all aerosol particle sizes. Uncertainties in Λ_{snow} caused by other parameters (snow particle number size spectrum, terminal velocity, and shape) can also be as large as one order of magnitude, whereas the corresponding uncertainties for Λ_{rain} are all smaller than a factor of 5.0. The combined uncertainty from all sources is thus larger for Λ_{snow} than for Λ_{rain}.

It has been speculated that snow particles might scavenge more aerosol particles than rain drops do for an equivalent precipitation amount given the larger surface areas and various shapes of snow particles (Reiter and Carnuth, 1969; Magono et al., 1975; Graedel and Franey, 1975; Murakami et al., 1985; Sparmacher et al., 1993; Croft et al., 2009; Kyrö et al., 2009). However, this hypothesis has not yet been verified by either field or theoretical studies. To shed some light on this issue, one simple approach would be to compare directly the magnitude of Λ_{snow} and Λ_{rain} profiles generated for the same precipitation amount. One challenge to this approach, though, is that both Λ_{snow} and Λ_{rain} have a large range of values and very large uncertainties.

A typical snowfall intensity (e.g., $1\,\mathrm{cm\,h^{-1}}$ of snow, which is approximately equivalent to $1\,\mathrm{mm\,h^{-1}}$ of liquid water) is chosen below as an example to compare the relative magnitudes of Λ_{snow} and Λ_{rain}. The minimum and maximum Λ_{snow} values (two blue lines) shown in Fig. 10 were extracted from all panels of Fig. 8 in the present study while those for Λ_{rain} (two red lines) were obtained from Fig. 8a of a previous study (Wang

ACPD
13, 14823–14869, 2013

et al., 2010). Λ_{snow} from the empirical formula of Paramonov et al. (2011) (shown in Fig. 8) and Λ_{rain} from an empirical formula plotted in Fig. 8a of Wang et al. (2010) are also depicted in Fig. 10 (two dashed lines).

It can be seen in Fig. 10 that uncertainties in (or ranges of) Λ_{snow} are up to two orders of magnitude for small (< 0.01 µm) and large aerosol particles (> 10 µm) and up to three orders of magnitude for median size aerosol particles. In comparison, uncertainties in Λ_{rain} are smaller than one order of magnitude for small and large aerosol particles and mostly smaller than two orders of magnitude for median size aerosol particles; the only exception for rain is for aerosol particles of 1–3 µm, for which the uncertainties are slightly higher than two orders of magnitude. It should be pointed out that part of the large range of Λ_{snow} values will be due to real variability (e.g., different snow particle shapes and related properties affecting Λ_{snow}) while the other part will be due to errors (e.g., improper formulation of related parameters). The median Λ_{snow} value seems to be a factor of 5–10 higher than the median Λ_{rain} value for most aerosol particle sizes, which suggests the possibility of faster removal of atmospheric aerosols by snow than by rain for an equivalent precipitation amount. However, almost all Λ_{rain} values lie within the range of Λ_{snow} values, which suggests that snow removal of aerosol particles may not always be faster than rain removal. The relative magnitudes of Λ_{snow} and Λ_{rain} should also depend on snow particle shape (see the minimum Λ_{snow} profiles in Fig. 8a and d) and other conditions that may not be explicitly considered in either Λ_{snow} or Λ_{rain} (e.g., Wang et al., 2011; Paramonov et al., 2011).

As discussed in Sect. 4.2, Λ_{snow} from the field-based empirical formula shown in Fig. 10 should be adjusted upwards to reflect the case of 1 mm h^{-1} precipitation intensity. This adjustment to the empirical Λ_{snow} profile would make it higher than the corresponding empirical Λ_{rain} profile for submicron aerosols. Thus, it is likely that snow removal is more effective than rain removal in many situations, although this conclusion may not apply to all snow particle shapes, to all aerosol particle sizes, or under all other conditions. A firm conclusion thus cannot be drawn at this stage due to the limited number of field and laboratory studies that are available as well as the large uncertainties in theoretical studies.

5 Conclusions

A review of current knowledge about Λ_{snow}, the size-resolved scavenging coefficient for atmospheric aerosols scavenged below cloud by falling snow, was conducted in this study. The four component parameters needed for theoretical formulations of Λ_{snow} all contribute significant uncertainties to the estimated Λ_{snow} values. As expected, the formulation of the collection efficiency E between snow particles and aerosol particles contributes the largest uncertainty to Λ_{snow} amongst all of the component parameters. However, uncertainties caused individually by the other parameters were also up to one order of magnitude, which was unexpectedly large in contrast to values obtained in an uncertainty analysis for Λ_{rain} presented in a previous study by Wang et al. (2010).

For a typical snowfall intensity of 1 mm h^{-1} (as liquid water equivalent, or approximately 1 cm h^{-1} of snow), the uncertainty associated with theoretically estimated Λ_{snow} profiles spans nearly three orders of magnitude, in contrast to the one to two order-of-magnitude range for Λ_{rain}. Moreover, most Λ_{rain} values lie in the lower end of the range of Λ_{snow} values, which suggests that snow scavenging of atmospheric aerosol particles is likely more effective than rain scavenging in many cases for an equivalent precipitation intensity. However, under certain circumstance (e.g., aerosol particle size, snow particle shape, snowfall and rainfall intensity), removal by snow might be slower than removal by rain. A complete picture cannot be drawn at the present time due to our limited knowledge.

Because of the large range of estimated Λ_{snow} and Λ_{rain} values, their close magnitudes, and their similar aerosol-particle-size dependent profiles, a simple semi-empirical formula for size-resolved Λ as a polynomial function of precipitation intensity might be appropriate for both Λ_{snow} and Λ_{rain}. Such a formula could be developed through curve-fitting over a wide range of precipitation conditions using the set of ex-

ACPD
13, 14823–14869, 2013

isting parameterizations and measurements reviewed in this and previous studies. The new parameterization could be implemented in any size-distributed particulate-matter model. This approach will be investigated in a separate study.

Appendix A

$N(D_p)$ from Scott (1982) (Table 2)

Scott (1982) assumed the snow particle number size distribution to follow the Marshall–Palmer (1948) distribution:

$$N(D_m) = N_{0e}\exp(-\beta_e D_m) \tag{A1}$$

where D_m is the actual snow particle size. In all of the calculations performed in this study, however, the equivalent diameter of the melted snow particles, D_p, was used. It was thus necessary to convert D_m to D_p for the Scott (1982) distribution.

Mass is conserved when a snow particle melts:

$$\rho_{water}\frac{\pi}{6}D_p^3 = \rho_{ice}\frac{\pi}{6}D_m^3 \tag{A2}$$

Here $\rho_{water} = 10^6\,\mathrm{g\,m^{-3}}$, and the ice density (i.e., frozen density) for a snow particle was calculated from an empirical formula of Holroyd (1971):

$$\rho_{ice} = \frac{170}{D_m} \quad (\mathrm{g\,m^{-3}}) \tag{A3}$$

Combining Eqs. (A2) and (A3), we then obtain

$$D_m = \frac{10^3}{\sqrt{170}}D_p^{3/2} \quad (\mathrm{m}) \tag{A4}$$

$$\mathrm{d}D_m = \frac{10^6}{170}\times\frac{3}{2}\times\frac{D_p^2}{D_m}\mathrm{d}D_p \quad (\mathrm{m}) \tag{A5}$$

ACPD
13, 14823–14869, 2013

The number of snow particles with a diameter between D_m to $D_m + dD_m$ in a unit volume of air, $N(D_m)dD_m$ can be expressed

$$N(D_m)dD_m = N_{0e} \exp\left(-\beta_e \frac{10^3}{\sqrt{170}} D_p^{3/2}\right) \times \frac{10^6}{170} \times \frac{3}{2} \times \frac{D_p^2}{D_m} dD_p \quad (m^{-3}) \tag{A6}$$

Here $N_{0e} = 5.0 \times 10^7$ (m^{-4}), $M = 0.37R^{0.94}$ ($g\,m^{-3}$), and $\beta_e = 2072M^{-0.33}$ (m^{-1}).

Appendix B

An empirical Λ_{snow} formula from Paramonov et al. (2011)

Paramonov et al. (2011) proposed a Λ_{snow} parameterization from the empirical fit of four years of field measurements in an urban environment in Helsinki, Finland:

$$\Lambda(d_p) = 10^{a_1 + a_2[\log_{10} d_p]^{-2} + a_3[\log_{10} d_p]^{-1}} + g \cdot (\mathrm{RH}) - h \tag{B1}$$

where d_p is particle diameter (in m), $a_1 = 28.0$, $a_2 = 1550.0$, $a_3 = 456.0$, $g = 0.00015$, $h = 0.00013$, and RH is relative humidity. The formula is only valid for aerosol particles of 0.01–1. µm in diameter and snowfall intensities of 0.1 to 1.2 mm h^{-1} (as liquid water equivalent). Nevertheless, the formula is applicable to snowfall episodes of snowflakes, snow grains, ice crystals, ice pellets, as well as mixed with rain.

References

Andronache, C., Grönholm, T., Laakso, L., Phillips, V., and Venäläinen, A.: Scavenging of ultrafine particles by rainfall at a boreal site: observations and model estimations, Atmos. Chem. Phys., 6, 4739–4754, doi:10.5194/acp-6-4739-2006, 2006.

Baklanov, A.: Parameterisation of the deposition processes and radioactive decay: a review and some preliminary results by the DERMA model, DMI Scientific Report 99-4, Danish Meteorological Institute, Copenhagen, Denmark, 1999.
Bell, D. A. and Saunders, C. P. R.: An experimental study of aerosol scavenging by hexagonal plate ice crystals, Atmos. Res., 38, 9–19, 1995.
Bohm, H. P.: A general equation for the terminal fall speed of solid hydrometeors, J. Atmos. Sci., 46, 2419–2427, 1989.
Bohm, H. P.: A general hydrodynamic theory for mixed-phase microphysics, Part 1: Drag and fall speed of hydrometeors, Atmos. Res., 27, 253–274, 1992.
Chate, D. M.: Study of scavenging of submicron-sized aerosol particles by thunderstorm rain events, Atmos. Environ., 39, 6608–6619, 2005.
Cotton, W. R., Stephens, M. A., Nehrkorn, T., and Tripoli, G. J.: The Colorado State University three-dimensional cloud/mesoscale model, Part 2: An ice phase parameterization, J. Rech. Atmos., 16, 295–319, 1982.
Croft, B., Lohmann, U., Martin, R. V., Stier, P., Wurzler, S., Feichter, J., Posselt, R., and Ferrachat, S.: Aerosol size-dependent below-cloud scavenging by rain and snow in the ECHAM5-HAM, Atmos. Chem. Phys., 9, 4653–4675, doi:10.5194/acp-9-4653-2009, 2009.
Dick, A. L.: A simple model for air/snow fractionation of aerosol components over the Antarctic Peninsula, J. Atmos. Chem., 11, 179–196, 1990.
Feng, J.: A 3-mode parameterization of below-cloud scavenging of aerosols for use in atmospheric dispersion models, Atmos. Environ., 41, 6808–6822, 2007.
Feng, J.: A size-resolved model for below-cloud scavenging of aerosols by snowfalls, J. Geophys. Res., 114, D08203, doi:10.1029/2008JD011012, 2009.
Field, P. R. and Heymsfield, A. J.: Aggregation and scaling of ice crystal size distributions, J. Atmos. Sci., 60, 544–560, 2003.
Field, P. R., Hogan, R. J., Brown, P. R. A., Illingworth, A. J., Choularton, T. W., and Cotton, R. J.: Parameterization of ice-particle size distributions for mid-latitude stratiform cloud, Q. J. Roy. Meteorol. Soc., 131, 1997–2017, 2005.
Gong, W., Dastoor, A. P., Bouchet, V. S., Gong, S. L., Makar, P. A., Moran, M. D., Pabla, B., Ménard, S., Crevier, L.-P., Cousineau, S., and Venkatesh, S.: Cloud processing of gases and aerosols in a regional air quality model (AURAMS), Atmos. Res., 82, 248–275, 2006.
Gong, W., Stroud, C., and Zhang, L.: Cloud processing of gases and aerosols in air quality modeling, Atmosphere, 2, 567–616, doi:10.3390/atmos2040567, 2011.

Graedel, T. E. and Franey, J. P.: Field measurements of submicron aerosol washout by snow, Geophys. Res. Lett., 2, 325–328, 1975.
Gunn, K. L. S. and Marshall, J. S.: The distribution with size of aggregate snowflakes, J. Meteorol., 15, 452–461, 1958.
Harimaya, T., Kodama, H., and Muramoto, K.: Regional differences in snowflake size distributions, J. Meteorol. Soc. Jpn., 82, 895–903, doi:10.2151/jmsj.2004.895, 2004.
Henzing, J. S., Olivié, D. J. L., and van Velthoven, P. F. J.: A parameterization of size resolved below cloud scavenging of aerosols by rain, Atmos. Chem. Phys., 6, 3363–3375, doi:10.5194/acp-6-3363-2006, 2006.
Heymsfield, A. J.: Properties of tropical and midlatitude ice cloud particle ensembles, Part 1: Median mass diameters and terminal velocities, J. Atmos. Sci., 60, 2573–2591, 2003.
Hobbs, P. V., Radke, L. F., Locatelli, J. D., Atkinson, D. G., Robertson, C. E., Weiss, R. R., Turner, F. M., and Brown, R. R.: Research Report VII, Dep. of Atmos. Sci., University of Washington, Seattle, Washington, USA, 1972.
Holroyd, E. W.: The meso and microscale structure of Great Lakes snowstorm bands, Ph.D. Dissertation,Albany, New York, USA, 1971.
Houze Jr., R. A., Hobbs, P. V., Herzegh, P. H., and Parsons, A. D.: Size distributions of precipitation particles in front clouds, J. Atmos.Sci., 36, 156–162, 1979.
Jiusto, J. E. and Bosworth, G.: Fall velocity of snow flakes, J. Appl. Meteorol., 10, 1352–1354, 1971.
Jylhä, K.: Relationship between the scavenging coefficient for pollutants in precipitation and the radar reflectivity factor, Part 1: Derivation, J. Appl. Meteorol., 38, 1421–1434, 1999.
Jylhä, K.: Removal by snowfall of emissions from a coal-fired power plant: observations and modelling, Water Air Soil Poll., 120, 397–420, 2000.
Knutson, E. D., Sood, S. K., and Stockham, J. J.: Aerosol collection by snow and ice crystals, Atmos. Environ., 10, 395–402, 1976.
Kyrö, E.-M., Grönholm, T., Vuollekoski, H., Virkkula, A., Kulmala, M., and Laakso, L.: Snow scavenging of ultrafine particles: Field measurements and parameterization, Boreal Environ. Res., 14, 527–538, 2009.
Laakso, L., Grönholm, T., Rannik, U., Kosmale, M., Fiedler, V., Vehkamäki, H., and Kulmala, M.: Ultrafine particle scavenging coefficients calculated from 6 years field measurements, Atmos. Environ., 37, 3605–3613, 2003.

Langleben, M. P.: The terminal velocity of snow aggregates, Q. J. Roy. Meteorol. Soc., 80, 174–181, 1954.

Lin, Y.-L., Farley, R. D., and Orville, H. D.: Bulk parameterization of the snow field in a cloud model, J. Clim. Appl. Meteorol., 22, 1065–1092, 1983.

Locatelli, J. D. and Hobbs, P. V.: Fall speeds and masses of solid precipitation particles, J. Geophys. Res., 79, 2185–2197, 1974.

Loosmore, G. A. and Cederwall, R. T.: Precipitation scavenging of atmospheric aerosols for emergency response applications: testing an updated model with new real-time data, Atmos. Environ., 38, 993–1003, 2004.

Magono, C., Endoh, T. and Itasaka, M.: Observation of aerosol particles attached to falling snow crystals, Journal of Faculty of Science of Hokkaido University, 4, 103–119, 1975.

Marshall, J. S. and Palmer, W. M.: The distribution of raindrop with size, J. Meteorol., 5, 165–166, 1948.

Martin, J. J., Wang, P. K., and Pruppacher, H. R.: A theoretical determination of the efficiency with which aerosol particles are collected by simple ice crystal plates, J. Atmos. Sci., 37, 1628–1663, 1980.

Maryon, R. H., Smith, F. B., Conwy, B. J., and Goddard, D. M.: The UK nuclear accident response model (NAME), Prog. Nucl. Energ., 26, 85–104, 1992.

Matson, R. J. and Huggins, A. W.: The direct measurement of sizes, shapes and kinematics of falling hailstones, J. Atmos. Sci., 37, 1107–1125, 1980.

Miller, N. L. and Wang, P. K.: Theoretical determination of the efficiency of aerosol particle collection by falling columnar ice crystals, J. Atmos. Sci., 46, 1656–1663, 1989.

Mitchell, D. L.: Evolution of snow-size spectra in cyclonic storms, Part 2: Deviations from the exponential form, J. Atmos. Sci., 45, 3431–3451, 1991.

Mitchell, D. L.: Use of mass- and area-dimensional power laws for determining precipitation particle terminal velocities, J. Atmos. Sci., 53, 1710–1723, 1996.

Mitchell, D. L. and Arnott, W. P.: A model predicting the evolution of ice particle size spectra and the radiative properties of cirrus clouds, Part 2: Dependencies of absorption and extinction on ice crystal morphology, J. Atmos. Sci., 51, 817–832, 1994.

Mitchell, D. L. and Heymsfield, A. J.: Refinements in the treatment of ice particle terminal velocities, highlighting aggregates, J. Atmos. Sci., 62, 1637–1644, 2005.

Mitchell, D. L., Zhang, R., and Pitter, R. L.: Mass-dimensional relationships for ice particles and the influence of riming on snowfall rates, J. Appl. Meteorol., 29, 153–163, 1990.

Molthan, A. L., Petersen, W. A., Nesbitt, S. W., and Hudak, D.: Evaluating the snow crystal size distribution and density assumptions within a single-moment microphysics scheme, Mon. Weather Rev., 138, 4254–4267, 2010.
Morrison, G., Thompson, G., and Tatarskii, V.: Impact of cloud microphysics on the development of trailing stratiform precipitation in a simulated squall line: comparison of one- and two-moment schemes, Mon. Weather Rev., 137, 991–1007, 2009.
Murakami, M., Magono, C., and Kikuchi, K.: Experiments on aerosol scavenging by natural snow crystals, Part 3: The effect of snow crystal charge on collection efficiency, J. Meteorol. Soc. Jpn., 63, 1127–1137, 1985.
Paramonov, M., Grönholm, T., and Virkkula, A.: Below-cloud scavenging of aerosol particles by snow at an urban site in Finland, Boreal Environ. Res., 16, 304–320, 2011.
Passarelli, R. E.: Theoretical and observational study of snow-size spectra and snowflake aggregation efficiencies, J. Atmos. Sci., 35, 882–889, 1978.
Pruppacher, H. R. and Klett, J. D.: Microphysics of clouds and precipitation, Kluwer Academic Publishers, Dordrecht, 954 pp., 1997.
Ranz, W. E. and Wong, J. B.: Impaction of dust and smoke particles, Ind. Eng. Chem., 44, 1371–1381, doi:10.1021/ie50510a050, 1952.
Rasch, P. J., Feichter, J., Law, K., Mahowald, N., Penner, J., Benkovitz, C., Genthon, C., Giannakopoulos, C., Kasibhatla, P., Koch, D., Levy, H., Maki, T., Prather, M., Roberts, D. L., Roelofs, G.-J., Stevenson, D., Stockwell, Z., Taguchi, S., Kritz, M., Chipperfield, M., Baldocchi, D., McMurry, P., Barrie, L., Balkanski, Y., Chatfield, R., Kjellstrom, E., Lawrence, M., Lee, H. N., Lelieveld, J., Noone, K. J., Seinfeld, J., Stenchikov, G., Schwartz, S., Walcek, C., and Williamson, D.: A comparison of scavenging and deposition processes in global models: results from the WCRP Cambridge Workshop of 1995, Tellus B, 52, 1025–1056, 2000.
Reisner, J., Rasmussen, R. M., and Bruintjes, R. T.: Explicit forecasting of supercooled liquid water in winter storms using the MM5 forecast model, Q. J. Roy. Meteorol. Soc., 124, 1071–1107, 1998.
Reiter, R. and Carnuth, W.: Washout-Untersuchungen an Fallout-Partikeln in der unteren Troposphäre zwischen 700 und 3000 m NN, Arch. Meteor. Geophy. A, 18, 111–146, 1969.
Rotstayn, L. D. and Lohmann, U.: Simulation of the tropospheric sulfur cycle in a global model with a physically based cloud scheme, J. Geophys. Res., 107, 4592, doi:10.1029/2002JD002128, 2002.

Rutledge, S. A. and Hobbs, P. V.: The mesoscale and microscale structure and organization of clouds and precipitation in midlatitude cyclones, Part 8: A model for the “seeder-feeder” process in warm-frontal rainbands, J. Atmos. Sci., 40, 1185–1206, 1983.
Santachiara, G., Prodi, F., and Belosi, F.: A review of termo- and diffusio-phoresis in the atmospheric aerosol scavenging process, Part 1: Drop scavenging, Atmos. Clim. Sci., 2, 148–158, 2012.
Sauter, D. P. and Wang, P. K.: An experimental study of the scavenging of aerosol particles by natural snow crystals, J. Atmos. Sci., 46, 1650–1655, 1989.
Scott, B. C.: Theoretical estimates of the scavenging coefficient for soluble aerosol particles as a function of precipitation type, rate and altitude, Atmos. Environ., 16, 1753–1762, 1982.
Seinfeld, J. H. and Pandis, S. N.: Atmospheric chemistry and physics: from air pollution to climate change, Wiley and Sons, New Jersey, 1203 pp., 2006.
Sekhon, K. S. and Srivastava, R. C.: Snow size spectra and radar reflectivity, J. Atmos. Sci., 27, 299–307, 1970.
Slinn, W. G. N.: Precipitation scavenging, in: Atmospheric Science and Power Production, chap. 11, edited by: Randerson, D., DOE/TIC-27601, US Department of Energy, Washington DC, 466–532, 1984.
Smith, P. L.: Equivalent radar reflectivity factors for snow and ice particles, J. Clim. Appl. Meteorol., 23, 1258–1260, 1984.
Sofiev, M., Siljamo, P., Valkama, I., Ilvonen, M., and Kukkonen, J.: A dispersion modelling system SILAM and its evaluation against ETEX data, Atmos. Environ., 40, 674–685, doi:10.1016/j.atmosenv.2005.09.069, 2006.
Solomon, A., Morrison, H., Persson, O., Shupe, M. D., and Bao, J. W.: Investigation of microphysical parameterizations of snow and ice in Arctic clouds during M-PACE through model-observation comparisons, Mon. Weather Rev., 137, 3110–3128, 2009.
Sparmacher, H., Fulber, K., and Bonka, H.: Below-cloud scavenging of aerosol particles: particle-bound radionuclides – experimental, Atmos. Environ. A-Gen., 27, 605–618, 1993.
Sportisse, B.: A review of parameterizations for modelling dry deposition and scavenging of radionuclides, Atmos. Environ., 41, 2683–2698, 2007.
Starr, D. O. and Cox, S. K.: Cirrus clouds, Part 1: A cirrus cloud model, J. Atmos. Sci., 42, 2663–2681, 1985.
Textor, C., Schulz, M., Guibert, S., Kinne, S., Balkanski, Y., Bauer, S., Berntsen, T., Berglen, T., Boucher, O., Chin, M., Dentener, F., Diehl, T., Easter, R., Feichter, H., Fillmore, D., Ghan, S.,

ACPD
13, 14823–14869, 2013

Assessment of scavenging coefficient formulations

L. Zhang et al.

Ginoux, P., Gong, S., Grini, A., Hendricks, J., Horowitz, L., Huang, P., Isaksen, I., Iversen, I., Kloster, S., Koch, D., Kirkevåg, A., Kristjansson, J. E., Krol, M., Lauer, A., Lamarque, J. F., Liu, X., Montanaro, V., Myhre, G., Penner, J., Pitari, G., Reddy, S., Seland, Ø., Stier, P., Takemura, T., and Tie, X.: Analysis and quantification of the diversities of aerosol life cycles within AeroCom, Atmos. Chem. Phys., 6, 1777–1813, doi:10.5194/acp-6-1777-2006, 2006.

Thompson, G., Rasmussen, R. M., and Manning, K.: Explicit forecasts of winter precipitation using an improved bulk microphysics scheme, Part 1: Description and sensitivity analysis, Mon. Weather Rev., 132, 519–542, 2004.

Thompson, G., Field, P. R., Rasmussen, R. M., and Hall, W. D.: Explicit forecasts of winter precipitation using an improved bulk microphysics scheme, Part 2: Implementation of a new snow parameterization, Mon. Weather Rev., 136, 5095–5115, 2008.

Tost, H., Jöckel, P., Kerkweg, A., Sander, R., and Lelieveld, J.: Technical note: A new comprehensive SCAVenging submodel for global atmospheric chemistry modelling, Atmos. Chem. Phys., 6, 565–574, doi:10.5194/acp-6-565-2006, 2006.

Wang, X., Zhang, L., and Moran, M. D.: Uncertainty assessment of current size-resolved parameterizations for below-cloud particle scavenging by rain, Atmos. Chem. Phys., 10, 5685–5705, doi:10.5194/acp-10-5685-2010, 2010.

Wang, X., Zhang, L., and Moran, M. D.: On the discrepancies between theoretical and measured below-cloud particle scavenging coefficients for rain – a numerical investigation using a detailed one-dimensional cloud microphysics model, Atmos. Chem. Phys., 11, 11859–11866, doi:10.5194/acp-11-11859-2011, 2011.

Woods, C. P., Stoelinga, M. T., and Locatelli, J. D.: Size spectra of snow particles measured in wintertime precipitation in the Pacific Northwest, J. Atmos. Sci., 65, 189–205, doi:10.1175/2007JAS2243.1, 2008.

Zhang, L., Michelangeli, D. V., and Taylor, P. A.: Numerical studies of aerosol scavenging in low-level, warm stratiform clouds and precipitation, Atmos. Environ., 38, 4653–4665, 2004.

Zhang, Y.: Online-coupled meteorology and chemistry models: history, current status, and outlook, Atmos. Chem. Phys., 8, 2895–2932, doi:10.5194/acp-8-2895-2008, 2008.

ACPD

13, 14823–14869, 2013

Table 1. List of semi-empirical formulas for $E(d_\mathrm{p}, D_\mathrm{p})$.

Source	Formulas
Slinn (1984)[a]	$E(d_\mathrm{p},\lambda) = (\frac{1}{\mathrm{Sc}})^{\alpha} + \left[1 - \exp(-(1 + Re_{\lambda}^{1/2}))\frac{(d_\mathrm{p}/2)^2}{\lambda^2}\right] + \left(\frac{\mathrm{St}-\mathrm{St}^*}{\mathrm{St}-\mathrm{St}^*+2/3}\right)^{3/2}$
Murakami et al. (1985)[b]	$E(d_\mathrm{p},D_\mathrm{m}) = \frac{48D_\mathrm{diff}}{\pi D_\mathrm{m} V_\mathrm{D}}(0.65 + 0.44\mathrm{Sc}^{1/3}\mathrm{Re}^{1/2}) + 28.5 I^{1.186} + \left(\frac{S_1 - S_2}{S_2\exp(S_1 t') - S_1\exp(S_2 t')}\right)^2$
Dick (1990)[c]	$E(d_\mathrm{p},D_\mathrm{m}) = \frac{2mV_\mathrm{D}}{3\pi d_\mathrm{p}\mu_\mathrm{a} D_\mathrm{m}} + \frac{4}{\mathrm{Pe}}(1 + 0.4Re^{1/6}\mathrm{Pe}^{1/3})$

[a] λ is the characteristic capture length and depends on the shape of snow particles (e.g., sleet/graupel, rimed crystals, powder snow, dendrite, tissue paper, and camera film). Re_λ is the Reynolds number corresponding to the specific λ. Sc is the Schmidt number: $\mathrm{Sc} = \mu_\mathrm{a}/\rho_\mathrm{a} D_\mathrm{diff}$, where μ_a is the dynamic air viscosity, ρ_a is the air density and D_diff is the aerosol-particle diffusion coefficient. St is the Stokes number and St* is the critical Stokes number: $\mathrm{St}^* = \frac{1.2+(1/12)\ln(1+Re_\lambda)}{1+\ln(1+Re_\lambda)}$.

[b] The formula is for snow aggregates. D_diff is the aerosol-particle diffusion coefficient, Re is the Reynolds number of a snow particle: $Re = D_\mathrm{m} V_\mathrm{D} \rho_\mathrm{a}/\mu_\mathrm{a}$, where ρ_a is the air density and μ_a is the dynamic air viscosity. Sc is the Schmidt number: $\mathrm{Sc} = \mu_\mathrm{a}/\rho_\mathrm{a} D_\mathrm{diff}$, and I is the size ratio $d_\mathrm{p}/D_\mathrm{c}$, with D_c the characteristic length of the snow particle. The third term is the theoretical solution of a simplified flow model by Ranz and Wong (1952), involving parameters S_1, S_2 and t', and can be simplified to $\exp\left(\frac{-0.11}{\mathrm{St}^{1/2}-0.25}\right)$ if $\mathrm{St} \geq 1/16$, or to 0 if $\mathrm{St} < 1/16$ (Feng, 2009), where St is the Stokes number.

[c] m is the aerosol particle mass, μ_a is the dynamic air viscosity, and Pe is the Peclet number: $\mathrm{Pe} = D_\mathrm{m} V_\mathrm{D}/D_\mathrm{diff}$, where D_diff is the aerosol-particle diffusion coefficient. Re is the Reynolds number: $Re = D_\mathrm{m} V_\mathrm{D} \rho_\mathrm{a}/2\mu_\mathrm{a}$, where ρ_a is the air density and μ_a is the dynamic air viscosity.

ACPD
13, 14823–14869, 2013

Table 2. List of exponential snow particle number size distributions. Actual snow particle size was used in Scott (1982) (see Table A1) whereas melted snow particle sizes were used in other formulas. R is precipitation intensity ($mm\,h^{-1}$) and M is precipitation water concentration ($g\,m^{-3}$).

Source	$N(D_p) = N_{0e}\exp(-\beta_e D_p)$ N_{0e} [cm^{-4}]	β_e [cm^{-1}]
Marshall and Palmer (1948)	0.08	$\beta_e = 41R^{-0.21}$
Scott (1982)	0.5	$M = 0.37R^{0.94}$ $\beta_e = 20.7M^{-0.33}$ $= 28.8R^{-0.31}$
Gunn and Marshall (1958)	$N_{0e} = 0.038R^{-0.87}$	$\beta_e = 25.5R^{-0.48}$
Sekhon and Srivastava (1970)	$N_{0e} = 0.025R^{-0.94}$	$\beta_e = 22.9R^{-0.45}$

ACPD
13, 14823–14869, 2013

Table 3. List of empirical and theoretical snow particle terminal velocity ($\mathrm{cm\,s^{-1}}$) formulas.

Source	Formula	Particle shape
Langleben (1954)	$V_\mathrm{D} = 207D_\mathrm{p}^{0.31}$	plane dendrite
Jiusto and Bosworth (1971)	$V_\mathrm{D} = 104.9D_\mathrm{m}^{0.206}$	plane dendrite
Locatelli and Hobbs (1974)	$V_\mathrm{D} = 64.8D_\mathrm{m}^{0.257}$	plane dendrite
Molthan et al. (2010)	$V_\mathrm{D} = 110.1D_\mathrm{m}^{0.145}$	plane dendrite
Jiusto and Bosworth (1971)	$V_\mathrm{D} = 153D_\mathrm{m}^{0.206}$	column
Matson and Huggins (1980)	$V_\mathrm{D} = 1145D_\mathrm{p}^{0.5}$	graupel
Mitchell (1996)	$V_\mathrm{D} = \frac{R_\mathrm{e}\mu_\mathrm{a}}{D_\mathrm{m}\rho_\mathrm{a}}$ $R_\mathrm{e} = \begin{cases} 0.04394X^{0.970}, & 0.01 < X \leq 10.0 \\ 0.06049X^{0.831}, & 10.0 < X \leq 585 \\ 0.2072X^{0.638}, & 585 < X \leq 1.56\times10^{5} \\ 1.0865X^{0.499}, & 1.56\times10^{5} < X \leq 10^{8} \end{cases}$	any shape
Mitchell and Heymsfield (2005)	$V_\mathrm{D} = a_v D_\mathrm{m}^{b_v}$, $R_\mathrm{e} = a_1 X^{b1}$, $m = \alpha D_\mathrm{m}^{\beta}$, $A = \gamma D_\mathrm{m}^{\sigma}$ $a_v = a_1\left(\frac{\mu_\mathrm{a}}{\rho_\mathrm{a}}\right)^{(1-2b_1)}\left(\frac{2\alpha g}{\rho_\alpha\gamma}\right)^{b1}$, $b_v = b_1(\beta-\sigma+2)-1$	any shape

Here D_p (cm) is the equivalent diameter of a melted snow particle and D_m (cm) is the maximum dimension of the frozen snow particle. X is the Best number, $X = \frac{2mg\rho_\mathrm{a}D_\mathrm{m}^2}{A\mu_\mathrm{a}^2}$. m and A are the mass and cross-sectional area of a snow particle, respectively. α, β, γ and σ are constants (see discussion in Sect. 2.1), a_1 and b_1 are described as functions of X (see Mitchell and Heymsfield, 2005).

Table 4. Snow particle shapes considered in this study and their mass and cross-sectional area formulas. D_m is the ice crystal maximum diameter (cm).

Snow particle shape	Mass $m = \alpha D_m^{\beta}$ [g]	Cross-sectional Area $A = \gamma D_m^{\sigma}$ [cm^2]
Spheres	$m = 0.0524 D_m^{3.00a}$	$A = 0.7854 D_m^{2.00a}$
Dendrites	$m = 0.0022 D_m^{2.19b}$	$A = 0.2285 D_m^{1.88c}$
Columns	$m = 0.0450 D_m^{3.00b}$	$A = 0.0512 D_m^{1.41d}$
Graupel	$m = 0.0490 D_m^{2.80e}$	$A = 0.5000 D_m^{2.00a}$

[a] Obtained from $m = \rho_s(\pi/6)D_m^3$ and $A = (\pi/4)D_m^2$, with $\rho_s = 0.1\,\mathrm{g\,cm^{-3}}$.
[b] From Woods et al. (2008)
[c] From Mitchell (1996) for "Aggregates of side planes"
[d] From Mitchell (1996) for "Rimed long columns"
[e] From Mitchell (1996) for "Lump graupel"

ACPD
13, 14823–14869, 2013

Table 5. Total snow particle number concentration (N_{total}, m^{-3}) for three of the number size distributions listed in Table 2 for four different snowfall intensities (as liquid water equivalent). MP denotes the Marshall and Palmer (1948) distribution, SC denotes the Scott (1982) distribution, and SS denotes the Sekhon and Srivastava (1970) distribution. f_1, f_2, and f_3 are the percentages of the snow particles with equivalent melted diameter smaller than 0.1 mm, between 0.1–1.0 mm, and larger than 1 mm, respectively.

R	MP				SC				SS			
(mm h^{-1})	N_{total} (m^{-3})	f_1 (%)	f_2 (%)	f_3 (%)	N_{total} (m^{-3})	f_1 (%)	f_2 (%)	f_3 (%)	N_{total} (m^{-3})	f_1 (%)	f_2 (%)	f_3 (%)
0.1	1126.5	46.4	53.4	0.2	8381.3	37.0	63.0	0.0	3164.7	45.4	54.3	0.2
1.0	1872.5	31.9	66.1	2.0	17 238.9	20.2	79.7	0.1	1066.1	19.3	69.5	11.2
5.0	2655.4	24.0	69.9	6.1	28 474.7	12.8	85.4	1.8	490.1	9.9	55.5	34.6
10.0	3083.2	21.1	70.0	8.9	35 332.7	10.5	85.6	3.9	349.9	7.3	46.7	46.0

ACPD
13, 14823–14869, 2013

Assessment of scavenging coefficient formulations

L. Zhang et al.

Table A1. Nomenclature.

a_v, b_v	empirical constants in V_D power-law relationships
A	snow-particle effective cross-sectional area projected normal to the fall direction (m^2)
d_p	aerosol particle diameter (m)
D_p	melted diameter of a snow particle (m)
D_m	maximum dimension of a snow particle (m)
D_c	snow-particle characteristic length used in E expression of Murakami et al. (1985) (m)
D_{diff}	aerosol-particle diffusivity coefficient ($m^2\,s^{-1}$)
$E(d_p, D_p)$	snow particle-aerosol particle collection efficiency
g	acceleration of gravity ($m\,s^{-2}$)
M	precipitation water concentration ($g\,m^{-3}$)
m	particle mass (kg)
$n(d_p, t)$	aerosol number concentration with diameters d_p at time t
N_{0e}	intercept parameter for exponential size distribution (m^{-4})
$N(D_p)$	snow particle number size distribution (m^{-4})
N_{total}	total number concentration of snow particles (m^{-3})
Pe	Peclet number
R	precipitation intensity ($mm\,h^{-1}$)
Re	Reynolds number
RH	relative humidity
Sc	Schmidt number
St	Stokes number
St^*	critical Stokes number
v_d	aerosol-particle terminal velocity ($m\,s^{-1}$)
V_D	snow-particle terminal velocity ($m\,s^{-1}$)
X	Davies number
α, β	empirical constants in mass-diameter power-law relationships
β_e	slope parameter for exponential size distribution
γ, σ	empirical constants in Area-diameter power-law relationships
λ	snow-particle characteristic capture length used in E expression of Slinn (1984) (m)
$\Lambda(d_p)$	size-resolved scavenging coefficient (s^{-1})
μ_a	dynamic air viscosity ($kg\,m^{-1}\,s^{-1}$)
ρ_a	air density ($kg\,m^{-3}$)
ρ_{water}	water density ($kg\,m^{-3}$)

ACPD
13, 14823–14869, 2013

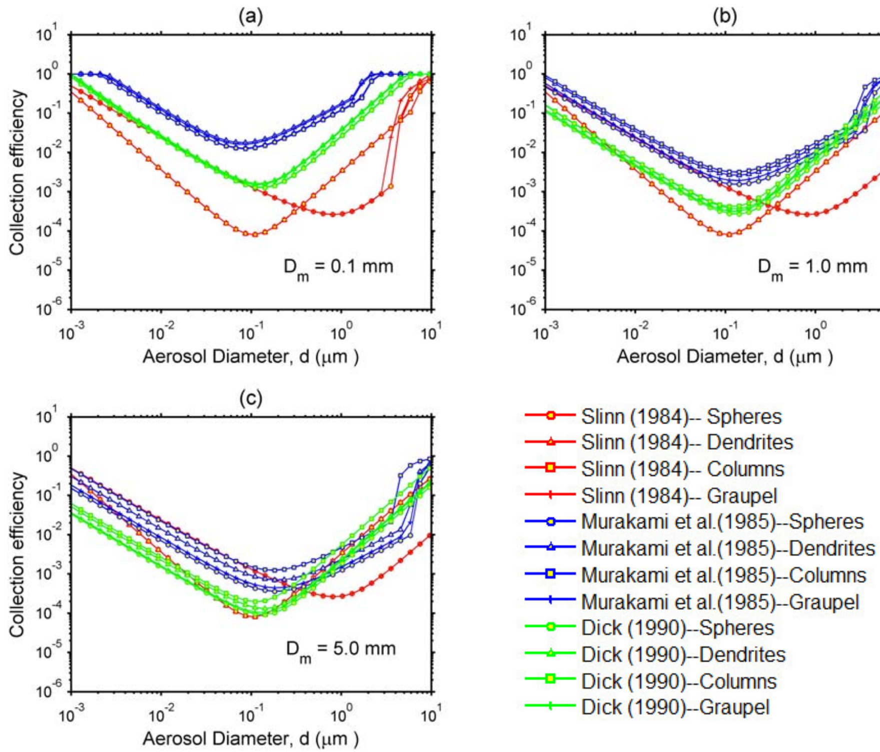

Fig. 1. Size-resolved snow collection efficiency profiles $E(d_p, D_p)$ calculated using the three formulas listed in Table 1 (three different colors) for aerosol particles from 0.001 to 10 μm in diameter collected by monodisperse snow particles of three different (frozen) sizes: **(a)** 0.1; **(b)** 1.0; and **(c)** 5.0 mm. Four different snow particle shapes are considered for each snow particle size (different symbols in each color group). Note in **(a)**, **(b)** and **(c)** the overlap of red triangle and red square and partially overlap of read circle and red cross; and in **(a)** the overlap of blue triangle and blue cross and the overlap of blue circle and blue square.

ACPD
13, 14823–14869, 2013

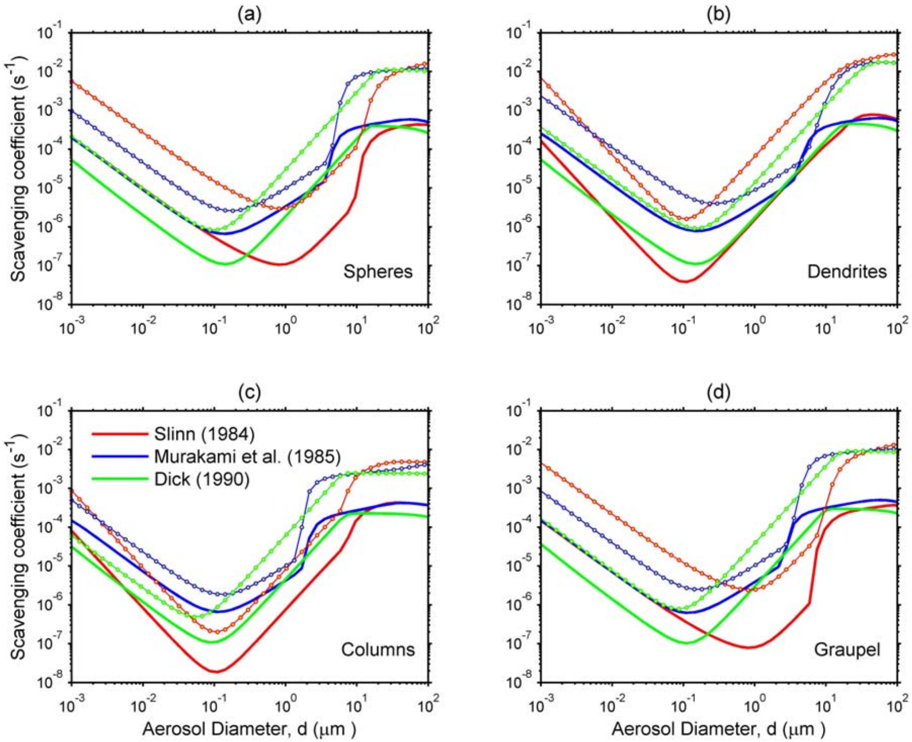

Fig. 2. Size-resolved snow scavenging coefficient profiles Λ_{snow} determined for three different $E(d_p, D_p)$ formulas (three different colors) under snowfall intensities of 0.1 (solid line) and 10.0 m h^{-1} (symbol line) for four snow particle shapes: **(a)** spheres; **(b)** dendrites; **(c)** columns; and **(d)** graupel.

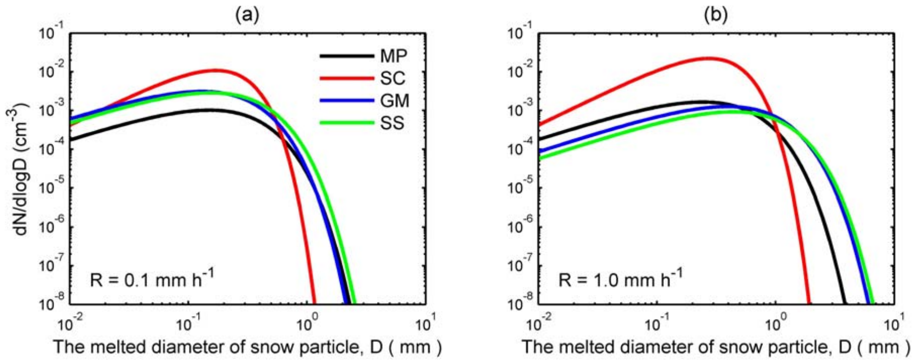

Fig. 3. Snow particle number size distributions under snowfall intensities (as liquid water equivalent) of **(a)** 0.1 mm h^{-1} and **(b)** 10.0 mm h^{-1} for four different formulas: MP – Marshall and Palmer (1948); SC – Scott (1982); GM – Gunn and Marshall (1958); and SS – Sekhon and Srivastava (1970).

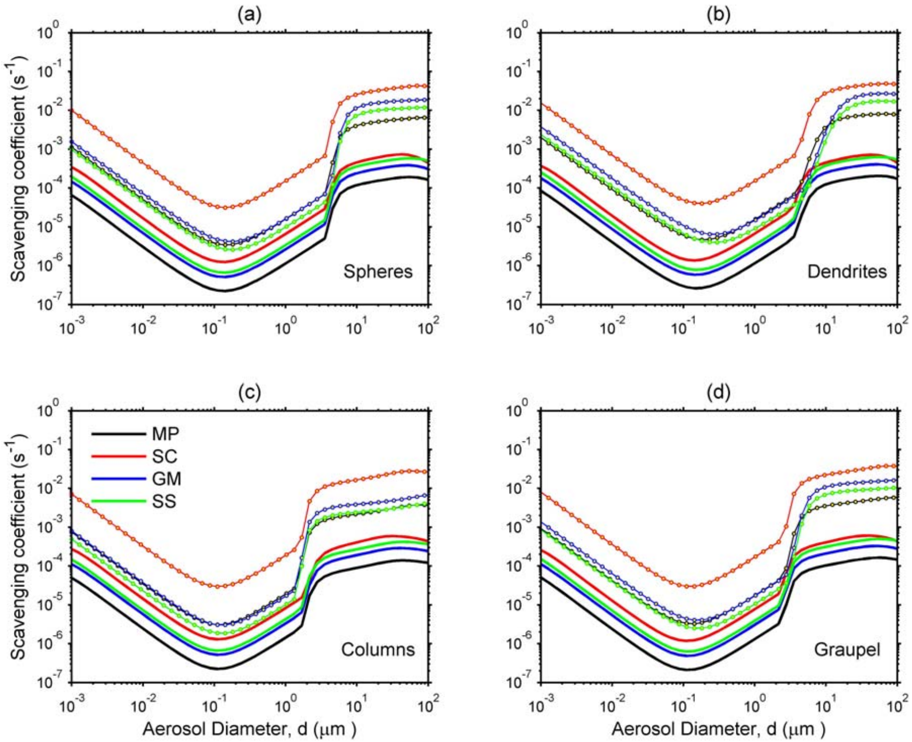

Fig. 4. Size-resolved snow scavenging coefficient profiles obtained using the four different snow particle number size distributions shown in Fig. 3 for snowfall intensities (as liquid water equivalent) of 0.1 (solid line) and 10 mm h^{-1} (symbol line) for four different snow particle shapes.

ACPD
13, 14823–14869, 2013

Title Page
Abstract | Introduction
Conclusions | References
Tables | Figures
◀| |▶
◀ ▶
Back | Close
Full Screen / Esc
Printer-friendly Version
Interactive Discussion

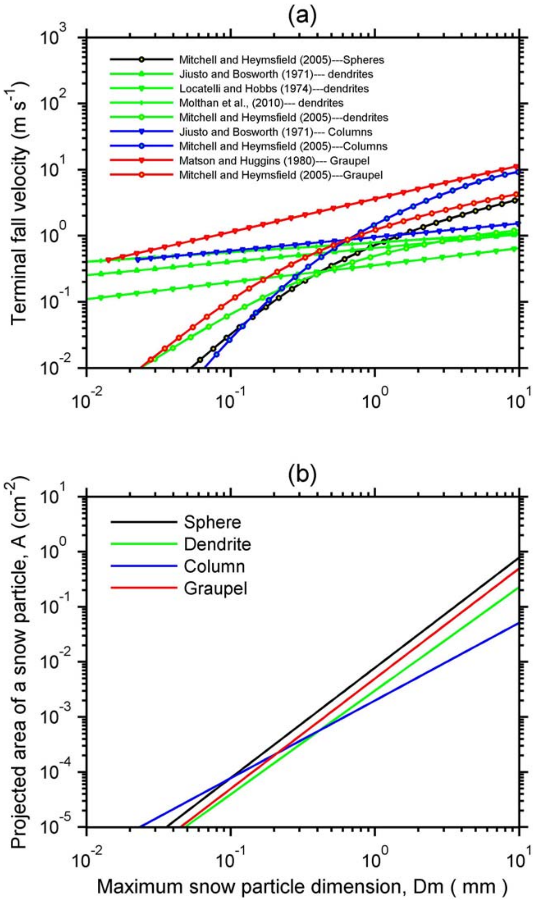

Fig. 5. Snow particle **(a)** terminal velocity and **(b)** cross-sectional area vs. maximum snow particle dimension derived from different parameterizations (see Tables 3 and 4).

ACPD
13, 14823–14869, 2013

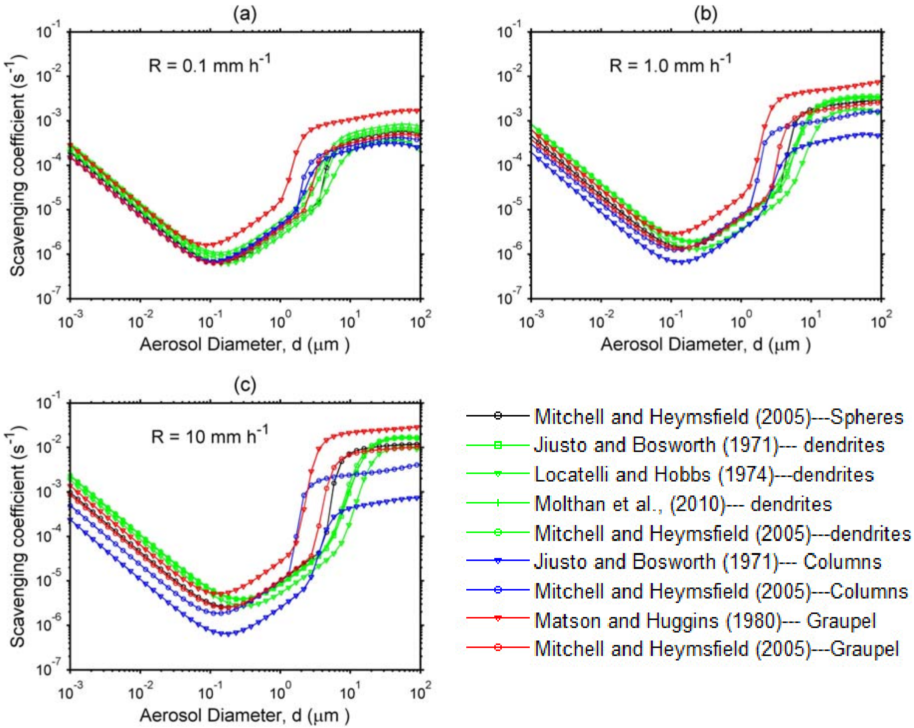

Fig. 6. Size-resolved snow scavenging coefficients Λ_{snow} derived from using different terminal velocity parameterizations for snowfall intensities (as liquid water equivalent) of **(a)** 0.1, **(b)** 1.0, and **(c)** 10 mm h^{-1}. Note that among the four green lines, the triangle one is at the bottom and the other three are close to each other.

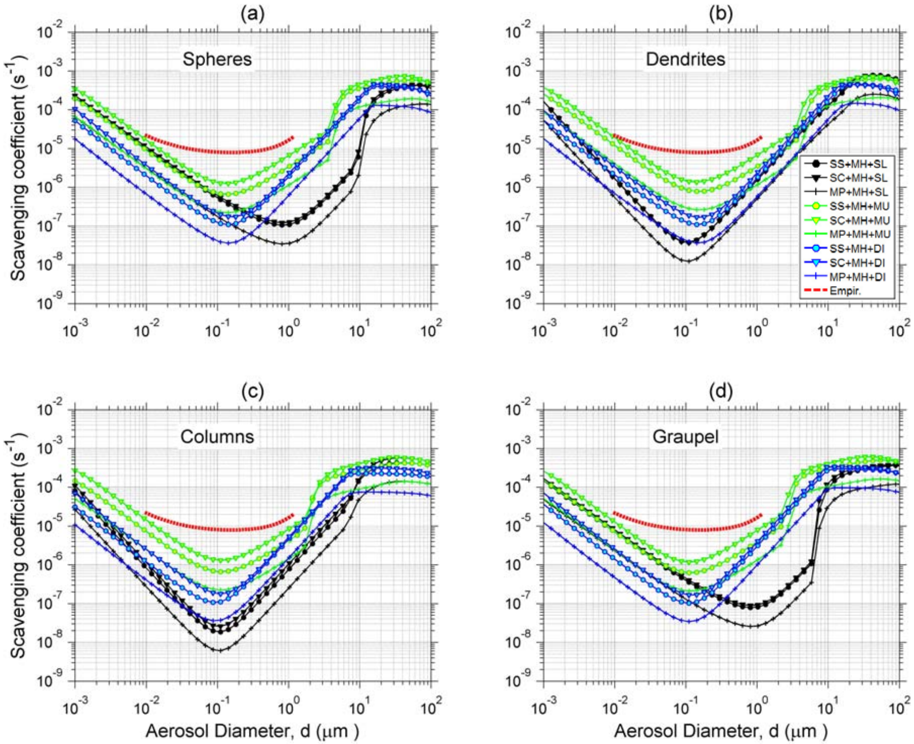

Fig. 7. Size-resolved Λ_{snow} profiles derived from nine theoretical parameterizations generated by a combination of three different $E(d_p, D_p)$ and three different $N(D_p)$ formulas for a snowfall intensity of 0.1 mm h^{-1} for four different snow particle shapes: **(a)** spheres; **(b)** dendrites; **(c)** columns; and **(d)** graupel. The following abbreviations are used: SS – Sekhon and Srivastava (1970); SC – Scott (1982); MP – Marshall and Palmer(1948); MH – Mitchell and Heymsfield (2005); SL – Slinn (1984); MU – Murakami et al. (1985); and DI – Dick (1990). Also shown is Empir. – Λ_{snow} calculated from Paramonov et al. (2011), which is only valid for aerosol particles with diameters between 0.01 and 1.0 μm.

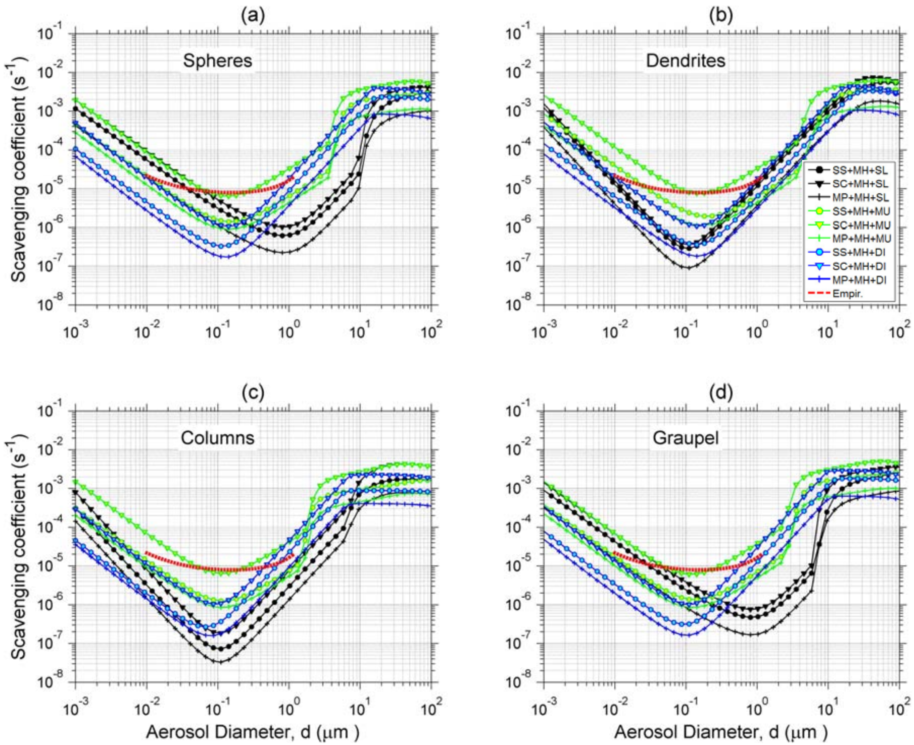

Fig. 8. Same as in Fig. 7 but for a snowfall intensity of 1.0 mm h^{-1} (note change in y-axis range).

ACPD
13, 14823–14869, 2013

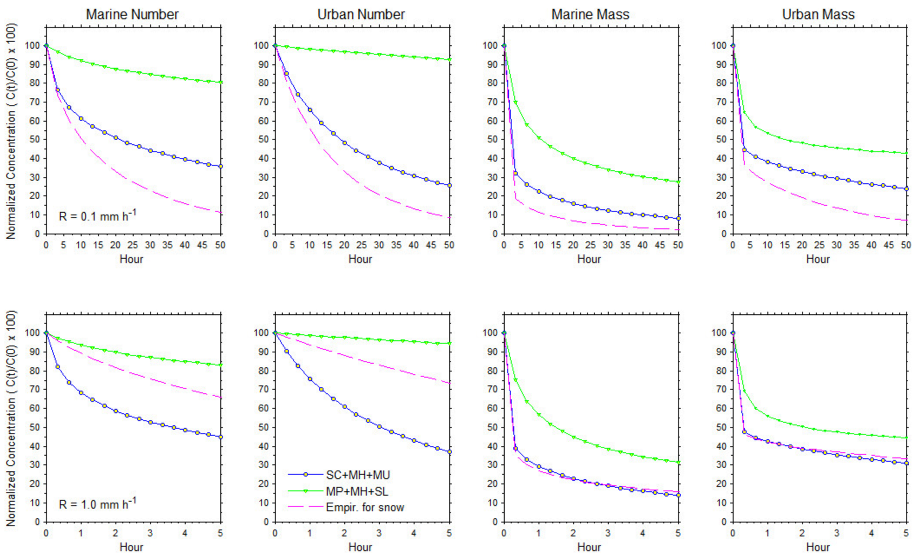

Fig. 9. Time evolution of normalized bulk aerosol number and mass concentrations for typical marine and urban aerosol populations under snow intensities of 0.1 and 1.0 mm h^{-1} (liquid water equivalent) calculated using two theoretical and one emipirical Λ_{snow} parameterizations shown in Figs. 7 and 8.

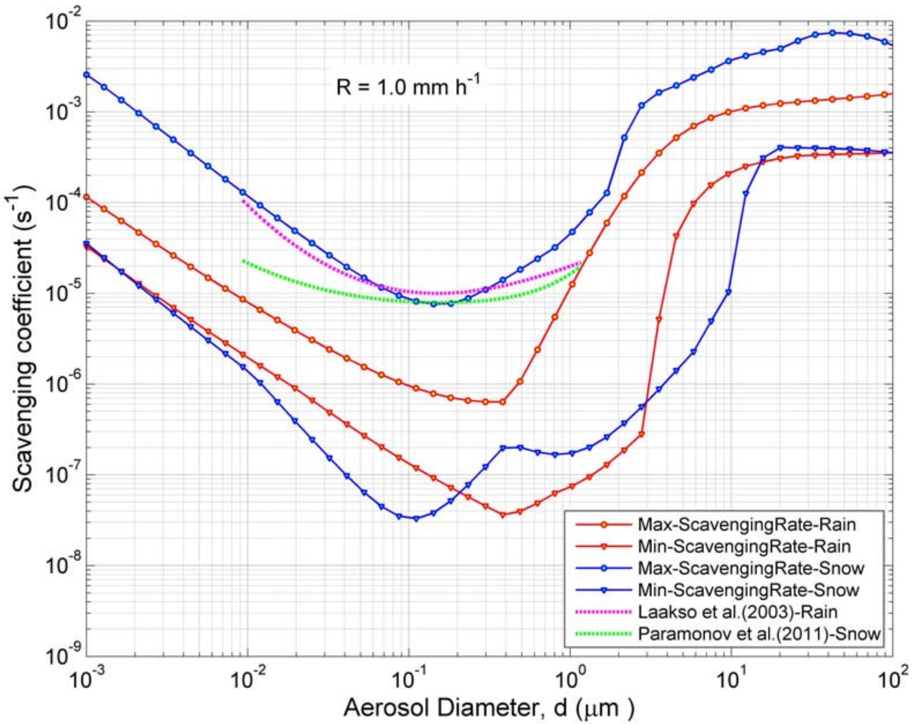

Fig. 10. The range (uncertainty) of Λ_{snow} and Λ_{rain} from existing theoretical formulations. Also shown are an empirical Λ_{snow} and an Λ_{rain} parameterization.